

University of Nebraska - Lincoln
DigitalCommons@University of Nebraska - Lincoln

Mechanical & Materials Engineering Faculty
Publications

Mechanical & Materials Engineering, Department
of

2015

The operation mechanism of poly(9,9-dioctylfluorenyl-2,7-diyl) dots in high efficiency polymer solar cells

Chunyu Liu
Jilin University

Yeyuan He
Jilin University


Xinyuan Zhang
Jilin University

Zhiqi Li
Jilin University

Liang Shen
University of Nebraska-Lincoln

See next page for additional authors

Follow this and additional works at: <http://digitalcommons.unl.edu/mechengfacpub>

 Part of the [Mechanical Engineering Commons](#), and the [Physical Sciences and Mathematics Commons](#)

Liu, Chunyu; He, Yeyuan; Zhang, Xinyuan; Li, Zhiqi; Shen, Liang; Zhang, Zhihui; Guo, Wenbin; and Ruan, Shengping, "The operation mechanism of poly(9,9-dioctylfluorenyl-2,7-diyl) dots in high efficiency polymer solar cells" (2015). *Mechanical & Materials Engineering Faculty Publications*. 120.
<http://digitalcommons.unl.edu/mechengfacpub/120>

This Article is brought to you for free and open access by the Mechanical & Materials Engineering, Department of at DigitalCommons@University of Nebraska - Lincoln. It has been accepted for inclusion in Mechanical & Materials Engineering Faculty Publications by an authorized administrator of DigitalCommons@University of Nebraska - Lincoln.

Authors

Chunyu Liu, Yeyuan He, Xinyuan Zhang, Zhiqi Li, Liang Shen, Zihui Zhang, Wenbin Guo, and Shengping Ruan

The operation mechanism of poly(9,9-dioctylfluorenyl-2,7-diyl) dots in high efficiency polymer solar cells

Chunyu Liu,¹ Yeyuan He,¹ Xinyuan Zhang,¹ Zhiqi Li,¹ Jinfeng Li,¹ Liang Shen,² Zhihui Zhang,¹ Wenbin Guo,^{1,a)} and Shengping Ruan¹

¹State Key Laboratory on Integrated Optoelectronics, Jilin University, 2699 Qianjin Street, Changchun 130012, China

²Department of Mechanical and Materials Engineering and Nebraska Center for Materials and Nanoscience, University of Nebraska–Lincoln, Lincoln, Nebraska 68588-0656, USA

(Received 19 March 2015; accepted 8 May 2015; published online 15 May 2015)

The highly efficient polymer solar cells were realized by doping poly(9,9-dioctylfluorenyl-2,7-diyl) (PFO) dots into active layer. The dependence of doping amount on devices performance was investigated and a high efficiency of 7.15% was obtained at an optimal concentration, accounting for a 22.4% enhancement. The incorporation of PFO dots (Pdots) is conducted to the improvement of J_{sc} and fill factor mainly due to the enhancement of light absorption and charge transport property. Pdots blended in active layer provides an interface for charge transfer and enables the formation of percolation pathways for electron transport. The introduction of Pdots was proven an effective way to improve optical and electrical properties of solar cells. © 2015 AIP Publishing LLC. [<http://dx.doi.org/10.1063/1.4921395>]

Polymer bulk heterojunction (BHJ) solar cells have achieved a continuing promise that demonstrate preferable performance of 6%–8% power conversion efficiencies.^{1–3} The BHJ is commonly implemented by casting a polymer:fullerene blend from solution, resulting in distributed junctions between the polymer donor and fullerene acceptor interfaces. Among numerous donor-acceptor groups, poly [N-9'-hepta-decanyl-2,7-carbazole-alt-5,5-(4',7'-di-2-thienyl-2'1',3'-benzothiadiazole)(PCDTBT):[6,6]-phenyl-C₇₁-butyric acid methyl ester (PC₇₀BM) blend has been widely employed into the fabrication of cell devices, demonstrating a high power conversion efficiency (PCE) of 10.2%.⁴ But it still lags behind the commercial application level and there are many challenges to overcome on the way to competitively efficient devices, including the need for a detailed knowledge of charge transport and spectrum utilization. Much effort have been made in recent years to pursue polymer solar cells exhibiting high PCE, such as designing low-bandgap organic semiconductor,^{5–7} developing novel device structure,^{8–10} and optimizing the film morphology.^{11–13} Although the perceived advantages of polymer solar cells are attractive, the efficiency of polymer solar cells (PSCs) is still limited by efficient hopping charge transport, and charge transport is further hindered by the presence of structural traps in the form of incomplete pathways in the percolation network. Different methods have been taken to enhance charge carrier mobility and charge collection efficiency without decreasing the thickness of active layer, so to avoid reduction of light absorption.^{14,15} Active layer doping has been proven an effective way to improve light harvesting and charge carrier transport of polymer solar cells.^{16,17} The presence of dopant in active layer provides an interface for charge transport. The additive can remove ubiquitous electron traps such as oxygen and enables

the formation of percolation pathways for charge transport. Introduction of dopants in active layer is easy to implement due to its simple process and low cost. Some organic molecules,^{18,19} metal nanoparticles (NPs),^{20,21} rare-earth NPs,^{22,23} and inorganic quantum dots^{24,25} have been doped into PSCs and further advanced their PCEs.

In this study, we doped poly(9,9-dioctylfluorenyl-2,7-diyl) (PFO) into PCDTBT:PC₇₀BM solution to fabricate active layer, and various concentrations were selected to optimize the cells performance. PFO was purchased from American Dye source and dissolved in tetrahydrofuran (THF) to obtain stock solutions of 1.0 mg/ml. A solution (3 ml) of PFO (80 ppm) was injected quickly into deionized water (10 ml) under sonication. The THF was removed by nitrogen (N₂) flowing under heating, followed by filtration through a 0.2 μm filter to remove larger aggregates, then concentrated by heating to get PFO dots (Pdots). The concentration of finally prepared Pdots solution was 1 mg/ml. Pdots solution of 5 μl, 10 μl, 20 μl, and 30 μl were added into each 1 ml 1,2-dichlorobenzene (DCB) solution composed of PCDTBT and PC₇₀BM, corresponding weight ratios (wt) of Pdots and PCDTBT:PC₇₀BM blend are 0.014 wt. %, 0.029 wt. %, 0.057 wt. %, and 0.086 wt. %, respectively. The devices with the structure of indium tin oxide (ITO)/nanocrystal titanium dioxide (nc-TiO₂)/PCDTBT:PC₇₀BM: Pdots/ molybdenum oxide (MoO₃)/silver (Ag) were prepared with different amounts of Pdots.^{26,27} The cells without and with 5 μl, 10 μl, 20 μl, and 30 μl PFO are named as devices A, B, C, D, and E, respectively.

As an initial study, we examine the influence of Pdots on the morphological properties of the photoactive layer. Figs. 1(a) and 1(b) show 1 μm × 1 μm Atomic Force Microscope (AFM) images of active layers without and with 0.029 wt. % Pdots. For pristine active layer, the film surface exhibits relatively smooth and featureless structure, which is similar to the observation reported previously.²⁸ Fig. 1(a)

^{a)}Author to whom correspondence should be addressed. Electronic mail: guowb@jlu.edu.cn.

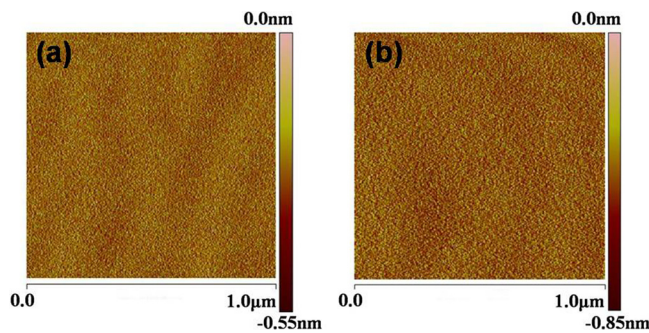


FIG. 1. AFM morphology images of active layer film (a) without Pdots, (b) doping with 0.029 wt. % Pdots.

displays a root-mean-square (RMS) roughness of 0.78 nm, and we observe an apparent surface reconstruction for doped film, whose RMS is around 0.96 nm. AFM results reveal that introducing Pdots in PCDTBT:PC₇₀BM blend leads to an obvious morphological variation. The diffuse reflection could occur on the rough surface of doped films, which is helpful to light trapping.

The current density-voltage (J-V) characteristics were measured with a computer-programmed Keithley 2400 source/meter with an Oriel 300 W solar simulator. Fig. 2 presents J-V characteristics of solar cells in our study. Detailed device parameters such as short-circuit current (J_{sc}), open-circuit voltage (V_{oc}), fill factor (FF), and PCE of devices doped with different amounts Pdots were summarized in Table I. It indicates that with the increase of doping amounts, PCEs of devices show a tendency of first increased and then decreased subsequently meanwhile reaching the maximum of 7.15% at the doping amount of 0.029 wt. %, exhibiting a J_{sc} of 14.30 mA/cm², a V_{oc} of 0.87 V, and a FF of 57.52%. Device A shows a J_{sc} of 12.96 mA/cm², a V_{oc} of 0.87 V, a FF of 51.8%, and a PCE of 5.84%. Comparing devices A and C, the higher efficiency of Device C is attributed to the increase of J_{sc} and FF. J_{sc} rises from 12.96 mA/cm² to 14.30 mA/cm² and FF raises from 51.8% to 57.5%, leading to a 22.4% PCE enhancement. For devices B, D, and E, high PCEs of 6.83%, 6.62%, and 6.30% were also obtained. Fig. 3 shows the incident photon-to-current conversion efficiency (IPCE) spectra of optimized devices. It can be seen that the IPCE of control

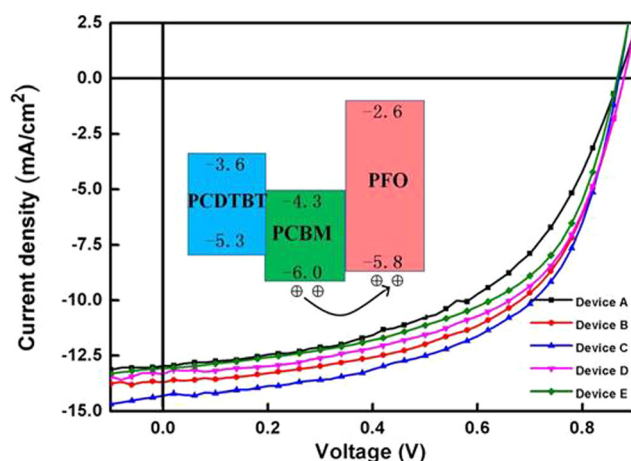


FIG. 2. J-V characteristics of devices doping with different concentrations of Pdots, inset is energy level of active layer materials.

TABLE I. Device performance, including open-circuit voltage (V_{oc}), short-circuit current density (J_{sc}), fill factor (FF), and power conversion efficiency (PCE), dependent on the different doping concentration of Pdots.

Device	V_{oc} (V)	J_{sc} (mA cm ⁻²)	FF (%)	PCE (%)
A	0.87	12.96	51.80	5.84
B	0.88	13.69	56.77	6.83
C	0.87	14.30	57.52	7.15
D	0.88	13.32	56.49	6.62
E	0.87	13.07	55.66	6.30

and doped cells is significantly different despite they possessed the same structure and experiment condition. The maximum IPCE value of 72% for doped cells appears at 460 nm, while that of the control device is 61% existing at 550 nm. The spectral response of the doped devices becomes stronger as a result of Pdots doping. Meanwhile, IPCE locating in the region of 350–550 nm is significantly enhanced. The net gain of light harvesting leads to significant photocurrent increase.

In order to verify how Pdots affects the optical property of doped devices, the absorption and reflection spectra of devices with different amounts of Pdots were measured first. Fig. 4(a) shows that the doped devices possess stronger absorbance than control device at the range of 300–1100 nm, and the absorption of doping cells also gradually enhances with the increase of Pdots. The following possible reason may explain the improved absorption resulting from incorporating Pdots, which is the optical path length in the active layer can be increased because light was trapped through multiple and high-angle scattering by Pdots. Fig. 4(b) demonstrates that the reflection of doping devices was significantly weakened, which is fairly consistent with Fig. 4(a). To explore charge carrier transport property of doped cells, we fabricated hole- and electron-only devices and the charge carrier mobilities were also calculated. The configuration of hole-only devices is ITO/MoO₃/PCDTBT: PC₇₀BM: Pdots/ MoO₃/Ag, where the MoO₃ connected with ITO is electron blocking layer. The structure of electron-only devices is ITO/TiO₂/PCDTBT: PC₇₀BM: Pdots/BCP/Ag, where the BCP is hole blocking layer. Both kinds of single charge

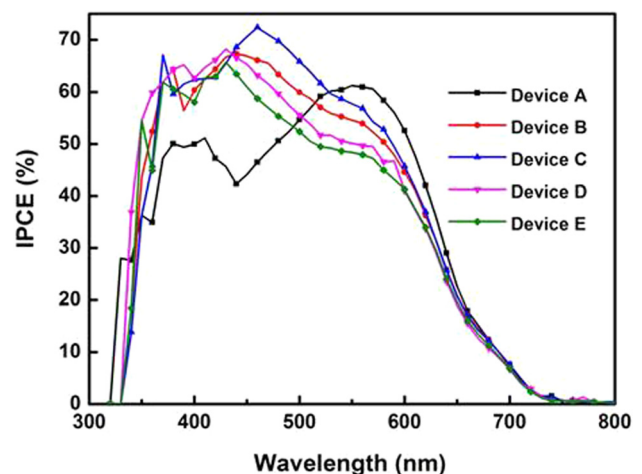


FIG. 3. IPCE spectra of inverted PSCs doping with different concentrations of Pdots.

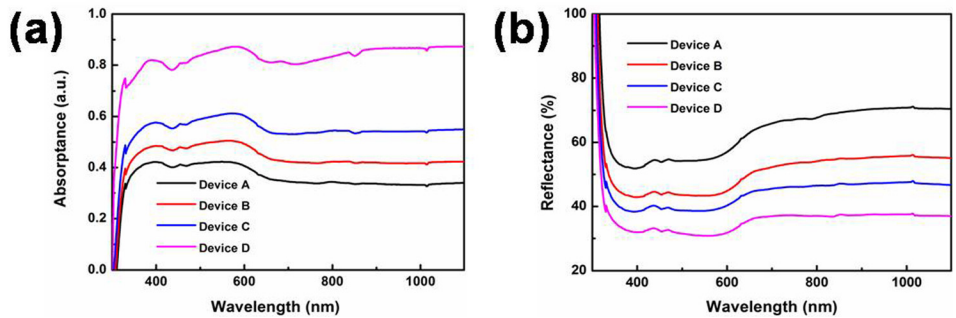


FIG. 4. The absorption and reflection spectra of completed devices doping with different concentrations of Pdots.

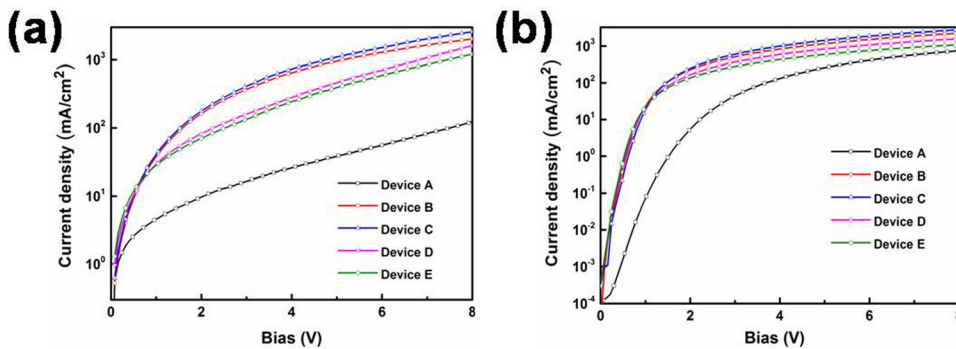


FIG. 5. J-V characteristics of single carrier device in dark (a) hole-only device and (b) electron-only device.

carrier devices were measured at the voltage range of 0–8 V in dark. Fig. 5 exhibits J-V characteristics of hole-only (Fig. 5(a)) and electron-only (Fig. 5(b)) devices. The current density of doped devices is larger than control device, and it is well agreement with the data in Fig. 2. The current density mainly depends on the directional movement of electrons under the driving bias in dark, so doped cells possess better capacity for electron transport. In order to make a realistic evaluation on the enhancement of charge transfer, charge carrier mobilities were calculated from space charge limited current (SCLC) model. At a typical applied voltage of 1.0 V, corresponding to an electric field of 10^5 V cm^{-1} across the bulk of a 100 nm active layer, apparent hole mobilities of $2.98 \times 10^{-5} \text{ cm}^2 \text{ V}^{-1} \text{ s}^{-1}$ and $1.42 \times 10^{-4} \text{ cm}^2 \text{ V}^{-1} \text{ s}^{-1}$ were got for devices without and with 0.029 wt. % Pdots doping, mobilities of other devices fall in between these two values and summarized in Table II.

To investigate the effect of Pdots on exciton generation and dissociation, dependence of the photocurrent density (J_{ph}) on the effective voltage (V_{eff}) on a double-logarithmic scale was investigated, which was shown in Fig. 6. J_{ph} is determined as $J_{ph} = J_L - J_D$, where J_L and J_D are the current density under illumination and in dark, respectively. V_{eff} is determined as $V_{eff} = V_0 - V$, where V_0 is the voltage at which $J_{ph} = 0$ and V is the applied bias voltage.²⁹ It is observed in Fig. 6 that J_{ph} linearly increases at a low value of V_{eff} , which tends to saturate at a sufficiently high value of V_{eff} . Assuming that all the photogenerated excitons are

dissociated into free charge carriers and collected by electrodes afterward at a high V_{eff} region,^{30,31} the result exhibits the free charge concentration of doping device is higher than control device, then saturation current density (J_{sat}) is only limited by total amount of absorbed incident photons. Meanwhile, the maximum exciton generation rate (G_{max}) could be calculated from $J_{sat} = e \times G_{max} \times L$, where e is the electron charge and L is the thickness of active layer. When an apparent enhancement of G_{max} occurred after Pdots incorporation, it suggested light trapping was greatly enhanced. In addition, J_{ph} increased faster for the doped device at low value of V_{eff} , indicating that Pdots addition made a positive effect on charge generation and dissociation.

A reasonable approach to overcome PCE limitation of low hole mobilities is to introduce high-mobility materials as additives in the active layers, which leads to the decrease in the injection barrier, making it less sensitive to the chosen

TABLE II. Hole and electron mobilities of devices doping with various concentrations Pdots.

Device	A	B	C	D	E
Hole	2.98×10^{-5}	2.59×10^{-4}	2.80×10^{-4}	1.95×10^{-4}	1.86×10^{-4}
Electron	1.27×10^{-6}	1.75×10^{-4}	1.42×10^{-4}	1.56×10^{-4}	1.62×10^{-4}

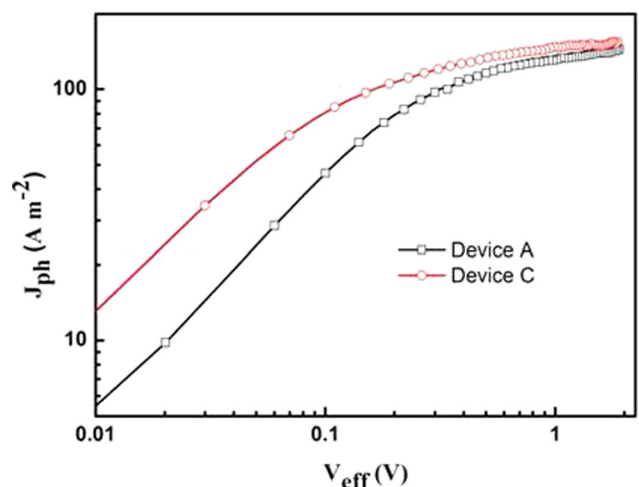


FIG. 6. Photocurrent density (J_{ph}) as a function of the effective voltage (V_{eff}) for control and doped devices under constant incident light intensity.

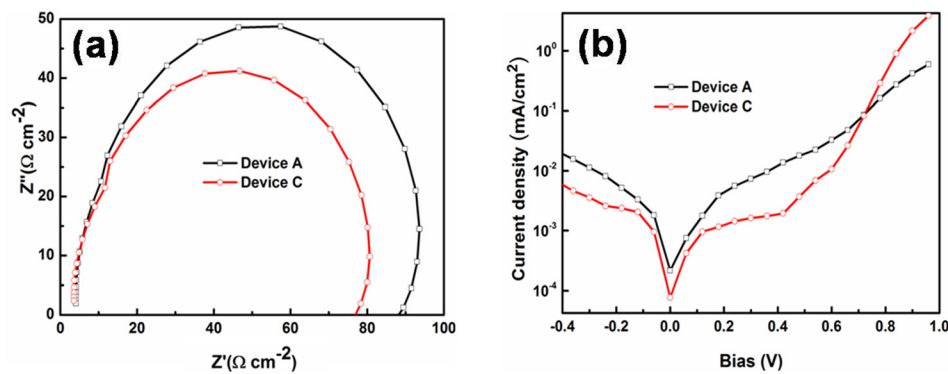


FIG. 7. (a) The J-V characteristics of devices without and with 0.029 wt. % Pdots in dark, (b) the impedance graph of PSCs devices without and with 0.029 wt. % Pdots in dark.

contact.³² The hole mobility of PFO is about $9.0 \times 10^{-3} \text{ cm}^2 \text{ V}^{-1} \text{ s}^{-1}$, which is two orders of magnitude higher than those of conventional PSCs, contributing to the increase of hole mobility in doped devices. At the same time, we can see that the highest occupied molecular orbital (HOMO) levels of PCDTBT and PFO are close and the energy difference is little, which can lead a pronounced enhancement of the hole mobility in the devices. The incorporation of PFO dots may increase the exciton generation rate and the dissociation probability in a low band gap PCDTBT:PC₇₁BM blend using molecular doping, by which interfacial recombination via charge transfer excitons is suppressed, leading to a high hole concentration.³³ High hole concentration will cause a strong local field and an obvious diffuse effect, which accelerate the transport rate of hole in the devices. The introduction of a little amount of Pdots can lead to a significant increase of the PCEs of PCDTBT/PC₇₁BM-based PSCs from 5.84% to 7.15%, which is mainly due to the remarkable increase in the hole mobilities of the devices.³⁴

Fig. 7(a) shows the dark current versus bias characteristics for devices A and C. The diode rectification ratio is apparently enhanced for Device C, indicating that doping significantly decreases the shunt resistance,³⁵ which contributes to the J_{sc} improvement. This suggests that the electron-dominant charge transport in active layer is drastically altered after adding Pdots. Fig. 7(b) exhibits the impedance of devices A and C with the frequency range from 20 Hz to 1 MHz, and series resistance of Device C reduced. It can be generally accepted that the injection barrier will decrease after doping of conducting polymers. As a result, the bias is mostly applied on the active layer than that on the resistance across the contacts. Lowering resistance undoubtedly helps reduce current losses across the contacting materials.³¹

In conclusion, Pdots doping in active layer has been investigated so as to re-visualize its effect on the performance improvement in PSCs. Under a doping concentration of 0.029 wt. %, the J_{sc} and FF for PCDTBT:PC₇₀BM based solar cells receives a considerable increase, leading to an ultimate enhancement of PCEs from 5.84% to 7.15%. We attribute the improvement to primarily increase of light absorption and charge carrier mobility. Meanwhile, resistance of finished devices and surface topography achieve an apparent improvement. All of these are beneficial for the efficiency enhancement of PSCs. Our results allow further insights into the role of polymer dopants in affecting the operation of PSCs.

Supported by National Natural Science Foundation of China (Nos. 61274068, 61077046, 61370046, and 51303061), 863 project (No. 2013AA030902), Project of Science and Technology Development Plan of Jilin Province (No. 20130206075SF), and the Open Fund of the State Key Laboratory on Integrated Optoelectronics (No. IOSKL2012KF03).

- ¹S. H. Park, A. Roy, S. Beaupre, S. Cho, N. Coates, J. S. Moon, D. Moses, M. Leclerc, K. Lee, and A. J. Heeger, *Nat. Photonics* **3**, 297 (2009).
- ²H. Y. Chen, J. Hou, S. Zhang, Y. Liang, G. Yang, Y. Yang, L. Yu, Y. Wu, and G. Li, *Nat. Photonics* **3**, 649 (2009).
- ³J. Hou, H.-Y. Chen, S. Zhang, R. I. Chen, Y. Yang, Y. Wu, and G. Li, *J. Am. Chem. Soc.* **131**, 15586 (2009).
- ⁴Z. C. He, C. M. Zhong, S. J. Su, M. Xu, H. B. Wu, and Y. Cao, *Nature Photon.* **6**, 591 (2012).
- ⁵Y. Y. Liang, Z. Xu, J. B. Xia, S. T. Tsai, Y. Wu, G. Li, C. Ray, and L. P. Yu, *Adv. Mater.* **22**, E135 (2010).
- ⁶C. Edwards, A. Arbabi, G. Popescu, and L. L. Goddard, *Light: Sci. Appl.* **1**, e30 (2012).
- ⁷T. Y. Chu, J. P. Lu, S. Beaupre, Y. G. Zhang, J. R. Pouliot, S. Wakim, J. Y. Zhou, M. Leclerc, Z. Li, J. F. Ding, and Y. Tao, *J. Am. Chem. Soc.* **133**, 4250 (2011).
- ⁸R. A. Taylor, T. Otanicar, and G. Rosengarten, *Light: Sci. Appl.* **1**, e34 (2012).
- ⁹Y. H. Su, Y. F. Ke, S. L. Cai, and Q. Y. Yao, *Light: Sci. Appl.* **1**, e14 (2012).
- ¹⁰J. Y. Kim, K. Lee, N. E. Coates, D. Mose, T. Q. Nguyen, M. Dante, and A. J. Heeger, *Science* **317**, 222 (2007).
- ¹¹X. N. Yang, J. Loos, S. C. Veenstra, W. J. H. Verhees, M. M. Wienk, J. M. Kroon, M. A. J. Michels, and R. A. Jassen, *Nano Lett.* **5**, 579 (2005).
- ¹²C. F. Guo, T. S. Sun, F. Cao, Q. Liu, and Z. F. Ren, *Light: Sci. Appl.* **3**, e161 (2014).
- ¹³S. J. Lou, J. M. Szarko, T. Xu, L. P. Lu, T. J. Marks, and L. X. Chen, *J. Am. Chem. Soc.* **133**, 20661 (2011).
- ¹⁴S. Liu, F. X. Meng, W. F. Xie, Z. H. Zhang, L. Shen, C. Y. Liu, Y. Y. He, W. B. Guo, and S. P. Ruan, *Appl. Phys. Lett.* **103**, 233303 (2013).
- ¹⁵D. Lepage, A. Jimenez, J. Beauvais, and J. J. Dubowski, *Light: Sci. Appl.* **1**, e28 (2012).
- ¹⁶L. Y. Lu, Z. Q. Luo, and L. P. Yu, *Nano Lett.* **13**, 59 (2013).
- ¹⁷D. H. Wang, D. Y. Kim, and K. W. Choi, *Angew. Chem.* **123**, 5633 (2011).
- ¹⁸C. W. Tang, *Appl. Phys. Lett.* **48**, 183 (1986).
- ¹⁹L. L. Huang, X. Z. Chen, B. F. Bai, Q. F. Tan, G. F. Jin, T. Zentgraf, and S. Zhang, *Light: Sci. Appl.* **2**, e70 (2013).
- ²⁰E. D. Kosten, J. H. Atwater, J. Parsons, A. Polman, and H. A. Atwater, *Light: Sci. Appl.* **2**, e45 (2013).
- ²¹A. Gole and C. J. Murphy, *Chem. Mater.* **17**, 1325 (2005).
- ²²C. Xiang, W. Koo, F. So, H. Sasabe, and J. Kido, *Light: Sci. Appl.* **2**, e74 (2013).
- ²³I. Hernandez, N. Pathumakanthar, P. B. Wyatt, and W. P. Gillin, *Adv. Mater.* **22**, 5356 (2010).
- ²⁴X. Chen, B. H. Jia, Y. A. Zhang, and M. Gu, *Light: Sci. Appl.* **2**, e92 (2013).
- ²⁵Z. Holman, S. Wolf, and C. Ballif, *Light: Sci. Appl.* **2**, e106 (2013).

- ²⁶C. Y. Liu, W. B. Guo, H. M. Jiang, L. Shen, S. P. Ruan, and D. W. Yan, *Org. Electron.* **15**, 2632 (2014).
- ²⁷Y. Y. He, C. Y. Liu, H. M. Jiang, W. B. Guo, L. Shen, and W. Y. Chen, *Synth. Met.* **195**, 117 (2014).
- ²⁸J. H. Seo, A. Gutacker, Y. M. Sun, H. B. Wu, F. Huang, Y. Cao, U. Scherf, A. J. Heeger, and G. C. Bazan, *J. Am. Chem. Soc.* **133**, 8416 (2011).
- ²⁹V. D. Mihailetchi, J. Wildeman, and P. W. M. Blom, *Phys. Rev. Lett.* **94**, 126602 (2005).
- ³⁰V. D. Mihailetchi, L. J. A. Koster, J. C. Hummelen, and P. W. M. Blom, *Phys. Rev. Lett.* **93**, 216601 (2004).
- ³¹C. G. Shuttle, R. Hamilton, B. C. O'Regan, J. Nelson, and J. R. Durrant, *Proc. Natl. Acad. Sci. U.S.A.* **107**, 16448 (2010).
- ³²S. H. Liu, P. You, J. H. Li, J. Li, C. S. Lee, B. S. Ong, C. Surya, and F. Yan, *Energy Environ. Sci.* **8**, 1463 (2015).
- ³³Y. Zhang, H. Q. Zhou, J. Seifert, L. Ying, A. Mikhailovsky, A. J. Heeger, G. C. Bazan, and T. Q. Nguyen, *Adv. Mater.* **25**, 7038 (2013).
- ³⁴F. Deschler, E. Da Como, T. Limmer, R. Tautz, T. Godde, M. Bayer, E. von Hauff, S. Yilmaz, S. Allard, U. Scherf, and J. Feldmann, *Phys. Rev. Lett.* **107**, 127402 (2011).
- ³⁵X. Liu, W. Wen, and G. C. Bazan, *Adv. Mater.* **24**, 4505 (2012).